International Journal of Thermophysics, Vol. 25, No. 6, November 2004 (© 2004)

High-Frequency Shear Modulus and Relaxation Time of Soft-Sphere and Lennard–Jones Fluids

E. Keshavarzi,[1] M. Vahedpour,[1] S. Alavi,[2,3] and B. Najafi[1]

Received November 18, 2003

The high-frequency shear modulus, G_∞, and shear relaxation time, τ_{shear}, are obtained using the Zwanzig–Mountain equation for soft-sphere and Lennard-Jones potentials. The Hansen and Weis soft-sphere radial distribution function and the Matteoli–Mansoori Lennard-Jones radial distribution function are used in the equation. The shear relaxation times of different isotherms for both of these fluids pass through a minimum at a reduced density of about 0.7, which indicates a change from fluid-like behavior to viscoelastic behavior. The origins of this common density point are discussed. It is also shown that for the Lennard-Jones fluid, if the ratio of the reduced relaxation time to a power of the reduced temperature is plotted as a function of the reduced density, all isotherms become superimposed on a single curve.

KEY WORDS: Lennard-Jones fluid; radial distribution function; shear modulus; shear relaxation time; soft-sphere fluid.

1. INTRODUCTION

Transport properties involve the flow of some quantity within a fluid system. Namely, viscosity involves the flow of the linear momentum, thermal conductivity the flow of thermal energy, and diffusion the flow of material in a mixture. This flow can result from local fluctuations inside an equilibrium system or from external driving forces in nonequilibrium systems [1].

In dilute-gas transport processes, the quantity being transported, such as linear momentum or energy, is carried by the individual molecules. For an ideal gas at thermal equilibrium, the distribution of molecular velocities is given by the Maxwell distribution law. In nonequilibrium states,

[1]Department of Chemistry, Isfahan University of Technology, Isfahan 84154, Iran.
[2]Department of Chemistry, University of Missouri-Columbia, Columbia, Missouri 65221, U.S.
[3]To whom correspondence should be addressed. E-mail: alavis@missouri.edu

0195-928X/04/1100-1747/0

the velocity distribution deviates from the Maxwell distribution, and the deviations are responsible for irreversible transport processes. If the deviation from the Maxwell distribution is known or can be calculated, the transport coefficient can be obtained. This is the basis of the Chapman–Enskog procedure [2] for deriving low-density transport coefficients for gases. The deviation from the Maxwell distribution is generally small when the system is not too far from equilibrium. If there is an external driving force, such as Poiseuille flow or a temperature gradient that prevents the attainment of equilibrium, the actual velocity distribution will be a compromise between the effect of this external influence and the rate with which collisions restore the Maxwell distribution [3]. The latter process can be characterized at each density and temperature by a "relaxation time," the calculation of which can be used to predict the transport coefficients.

The objective of this paper is to investigate the general behavior of the infinite-frequency shear modulus and shear relaxation time for soft-sphere (SS) and Lennard-Jones (LJ) fluids. The fundamental ideas originate with the Maxwell shear relaxation time, τ, that is defined as

$$\tau = \frac{\eta}{G_\infty}, \tag{1}$$

where η and G_∞ are the shear viscosity and high-frequency shear modulus, respectively.

When a mechanical force is suddenly applied to a fluid, the fluid initially responds elastically, as if it were a rigid, solid body. The initial response may be described by two quantities, the high-frequency limit of the shear modulus (or modulus of rigidity), G_∞, and the high frequency limit of the bulk modulus K_∞ (or modulus of compression).

Using a simple hydrodynamic model in which the molecule is regarded as a sphere rotating in a continuous viscous medium, Debye [4] found that the molecular relaxation time τ should be linearly dependent upon the viscosity η of the medium. Other workers [4] have proposed modified relationships, which are either based upon theoretical models or are purely empirical. Some of the empirical equations are quite successful in predicting the magnitude of relaxation times at room temperature for several polar liquids (such as nitrobenzene), which have viscosities in the range of 0.3–200 cP (1 cP = 10^{-3} Pa·s). However, but most empirical relations retain the linear dependence of τ upon η which is generally not observed. Hanley et al. [5], Hess and coworkers [6–8], and Mountain and Zwanzig [9] used radial distribution functions in the theoretical expression for the relaxation time, and van der Gulik [10] used the thermal pressure to calculate the shear relaxation time. Hill [11] obtained a theoretical relationship by beginning with Andrade's theory of viscosity and extending it to the case

of mixtures of liquids. From this she extracted a local viscosity that acts between species at the molecular level. The relaxation time depends upon this "mutual viscosity."

The shear viscosity relaxation time can be used to determine the elastic behavior (fluid-like or solid-like) of matter. The resistance to flow in fluids is characterized by the shear viscosity, and the elastic deformation in solids is characterized by the shear modulus. Intuitively, fluids readily flow under stress while solids do not. However, for short observation time, fluids may show elastic behavior. Similarly, for long observation time, solids may exhibit flow behavior. Whether a material flows or not depends on the dimensionless ratio (τ/t), which is called the Deborah number [12, 13], where t is the observation time (characteristic time scale of the flow) and τ is an average stress relaxation time of the material which is given by Eq. (1). If $t \ll \tau$, flow is not observed and the system exhibits solid-like behavior and satisfies Hooke's law. If $t \gg \tau$, flow is observed and the system exhibits fluid-like behavior and satisfies Newton's law of viscosity. For $t \approx \tau$, a material will show both elastic deformation and flow and is called viscoelastic. Viscoelastic behavior is commonly observed in polymer systems.

In our approach, we obtained expressions for the shear modulus G_∞ which are used to study the behavior of the relaxation time τ for SS and LJ supercritical fluids. It was observed that the variation of the relaxation time with density passes through a minimum at a reduced density $\rho^* \approx 0.65$ for argon and 0.7 for LJ and SS fluids. This trend may be attributed to a change from fluid-like to viscoelastic behavior in the supercritical region.

In Section 2 of this paper, we study the temperature and density dependence of the shear modulus for the SS potential. The shear relaxation time is determined from the shear modulus and values of the viscosity of the SS fluid. In Section 3, the density and temperature dependence of the shear modulus of a LJ fluid are determined. Viscosity values for the LJ fluid and argon are used to calculate the shear relaxation times of these two fluids. The paper ends in with a summary and discussion in Section 4.

2. CORRELATION FUNCTIONS FOR THE INFINITE-FREQUENCY SHEAR MODULUS AND RELAXATION TIMES OF SOFT-SPHERE FLUIDS

Zwanzig and Mountain [14] have derived the relation between the infinite-frequency shear modulus G_∞ and the radial distribution function

(RDF) for fluids interacting with a spherically symmetric potential,

$$G_\infty = \rho kT + \frac{2\pi}{15}\rho^2 \int_0^\infty g(r)\frac{d}{dr}\left[r^4 \frac{d\Phi(r)}{dr}\right] dr, \tag{2}$$

where $g(r)$, $\Phi(r)$, and ρ are the radial distribution function, intermolecular pair potential, and density, respectively, and kT has its usual meaning.

2.1. Shear Modulus for the Inverse Power Potential

A repulsive inverse power potential of order n is written as

$$\Phi = 4\varepsilon\left(\frac{\sigma}{r}\right)^n, \tag{3}$$

where σ is an effective radius and ε is the energy factor. Substituting the derivatives of Φ in the expression for G_∞ gives

$$G_\infty = \rho kT + 4n(n-3)\varepsilon\sigma^2\rho^2\frac{2\pi}{15}\int_0^\infty g(r)\left(\frac{\sigma}{r}\right)^{n-2} dr. \tag{4}$$

Heyes and Aston [15] demonstrate that the integral in Eq. (4) (and therefore G_∞) is infinite for a hard sphere potential with $n \to \infty$. However, this integral is finite for the soft-sphere repulsive potential with $n = 12$ and can be solved numerically for this important case.

It has been demonstrated [16–18] that the partition function and therefore, some thermodynamic properties of a SS fluid scale with a single variable, $x = \rho\sigma^3(\varepsilon/(kT))^{3/n}$. Hansen and Weis [16] have tabulated $g(r)$ for the SS fluid with $n = 12$ as a function of x. We have solved Eq. (4) numerically for $G^*_\infty = G_\infty\sigma^3/\varepsilon$ at several thermodynamic states using the SS potential and $g(r)$ from Ref. 16. Figure 1 shows G^*_∞ as a function of the reduced density $\rho^* = \rho\sigma^3$ for four isotherms. The scaling properties of the RDF suggest that by combining the reduced variables G^*_∞, ρ^*, and $T^* = kT/\varepsilon$, we can define

$$y \equiv \frac{G^*_\infty - \rho^* T^*}{\rho^{*2}} = 4n(n-3)\frac{2\pi}{15}\int_0^\infty g(r)\left(\frac{\sigma}{r}\right)^{n-2} d\left(\frac{r}{\sigma}\right). \tag{5}$$

The quantity y is proportional to the integral of Eq. (5) which scales with x. Therefore, it is possible to express y as a function of x for different thermodynamic states. The data for several isotherms can be summarized

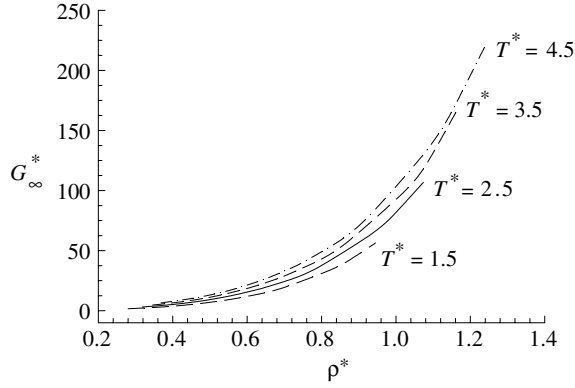

Fig. 1. Reduced soft-sphere shear modulus, $G_\infty^* = G_\infty \sigma^3/\varepsilon$, as a function of reduced density for several isotherms.

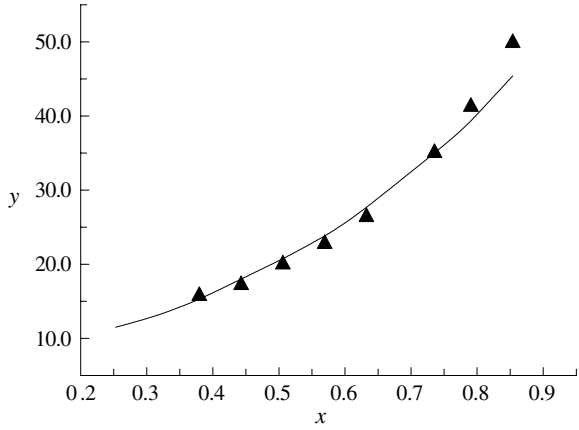

Fig. 2. Dimensionless variable y defined in Eq. (5) as a function of x. Molecular dynamic results (▲) of Heyes [19] are also given.

in a single curve by plotting the shear modulus in the form of y as a function of x. In Fig. 2 we show the good agreement between the results of Eq. (5) and the SS potential molecular dynamic simulations of Heyes [19].

The dependence of the variable y on x can be fit to the following functional form:

$$y = -1.6126 + 7.5828e^{2.1429x}. \tag{6}$$

This form is valid in the range of $0.253 < x < 0.854$ which is the range of the data for g(r) given in Ref. 16. With this simple functional form, G^*_∞ can be calculated for different values of ρ^* and T^*. The mean and maximum percent error for this fitting function are 0.48 and 1.14%, respectively.

2.2. Soft-Sphere Relaxation Time

With numerical integration of Eq. (5) or use of the functional form given in Eq. (6), G^*_∞ for the SS potential can be calculated and it becomes possible to determine the shear relaxation time. To do this, we use Eq. (6) for G^*_∞ and the Ashurst–Hoover [20] expression for reduced shear viscosity, $\eta^* = \eta\sigma^2/(m\varepsilon)^{1/2}$ of a soft sphere fluid. The Ashurst–Hoover expression for shear viscosity of a SS fluid in reduced form is

$$\eta^* = 0.171 + 0.022^* T^{*2/3} \left(e^{6.83x} - 1\right). \tag{7}$$

Substituting Eqs. (6) and (7) in Eq. (1), the reduced shear relaxation time for the soft sphere fluid can be calculated. The reduced shear relaxation time τ^*_{shear}, is defined as

$$\tau^*_{\text{shear}} = \frac{\tau_{\text{shear}}}{\sigma(m/\varepsilon)^{1/2}}. \tag{8}$$

The reduced shear relaxation times as a function of reduced density for three isotherms are plotted in Fig. 3, where it is seen that all isotherms pass through a minimum. The origin of this minimum is discussed in Section 4.

3. CORRELATION FUNCTION FOR THE SHEAR MODULUS AND RELAXATION TIME OF LENNARD–JONES FLUIDS

There are several semiemperical and analytical expressions for the shear modulus and viscosity for LJ fluids [19,21–23], but there are few data and no unique formula for the predicting the relaxation times.

3.1. LJ Shear Modulus

To obtain the shear modulus for the LJ potential, the integral in Eq. (2) is evaluated numerically using the RDF of pure LJ fluids given by

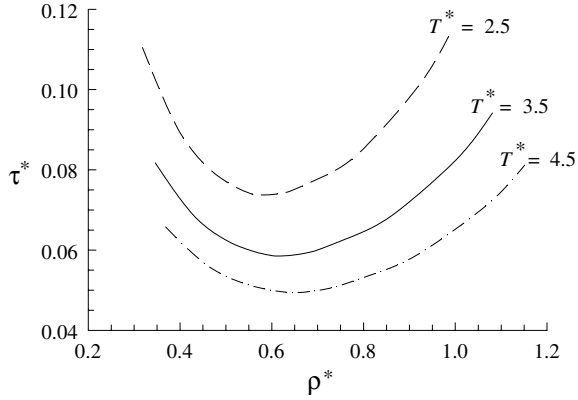

Fig. 3. Reduced shear relaxation time for a SS fluid as a function of the reduced density for several isotherms.

Matteoli and Mansoori [24]. Their expression is

$$g(y) = 1 - y^{-m}[g(d) - 1 - \lambda] + [(y - 1 + \lambda)/y] \times \{\exp[-\alpha(y-1)]\cos[\beta(y-1)]\}, \quad m \geqslant 1, \quad y \geqslant 1 \tag{9}$$

$$g(y) = g(d)\exp[-\theta(y-1)^2], \quad y < 1,$$

where $y = r/d$ is the dimensionless intermolecular distance, d is the location of the maximum of the first peak in the radial distribution function, and $h = d/\sigma, m, \lambda, \alpha, \beta, \theta$, and $g(d)$ are adjustable parameters. This expression for $g(r)$ is valid in the range of $0.25 < \rho^* < 0.95$ and $1.35 < T^* < 3.7$. Hence, the calculated G^*_∞ will be accurate in this region.

Figure 4 shows G^*_∞ for LJ fluids obtained from numerical solution of Eq. (2). Molecular dynamics (MD) results for LJ fluids [19,21] for two isotherms are also shown. The agreement between our predictions and the MD results is acceptable.

For practical purposes, it is convenient to fit the calculated G^*_∞ in the reduced density range of $0.25 \leqslant \rho^* \leqslant 0.95$ and reduced temperature range of $1.35 \leqslant T^* \leqslant 3.7$ to a functional form. The following form was used:

$$G^*_\infty = -0.6848 + (4.0478 + 13.1041T^*)\rho^{*1.7973} + (41.084 - 5.5881T^*)\rho^{*3.5814}, \tag{10}$$

where the adjustable parameters are obtained by a least-squares fitting method. The maximum relative percent error and the average relative percent error of this correlation for 100 points are 5.5 and 1.6%, respectively.

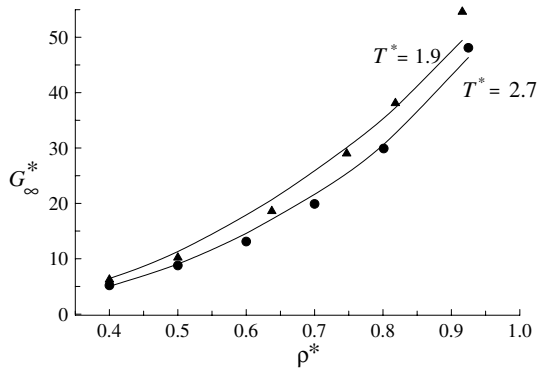

Fig. 4. Comparisons of the infinite-frequency shear modulus for the LJ fluid using the numerical solution of Eq. (2) and MD calculations for $T^* = 1.9(\blacktriangle)$ and $T^* = 2.7(\bullet)$ for two isotherms.

3.2. LJ Shear Relaxation Time

To obtain the shear relaxation time of LJ potentials, we use the analytical expression for reduced shear viscosity of LJ (supercritical) fluids given by Rowley and Painter [25]

$$\eta^* = \eta_0^* \exp\left[\sum_{i=1}^{4}\sum_{j=1}^{6} b_{ji}\frac{\rho^{*i}}{T^{*j-1}}\right], \tag{11}$$

where η_0^* is the reduced Chapman–Enskog low density viscosity,

$$\eta_0^* = \frac{5}{16}\sqrt{\frac{T^*}{\pi}}\left(\sum_{j=1}^{5}\omega_j T^{*j-1}\right)^{-1}, \tag{12}$$

and adjustable parameters b_{ji} and ω_j are given in Table I. This equation spans the range of $0 \leqslant \rho^* \leqslant 1.0$ and $0.8 \leqslant T^* \leqslant 4.0$.

The reduced relaxation time for LJ fluids may be obtained from the reduced form of Eq. (1)

$$\tau^* = \frac{\eta^*}{G_\infty^*}, \tag{13}$$

where η^* is substituted from Eq. (11) and G_∞^* from numerical solution of Eq. (2). In Fig. 5 the reduced shear relaxation time of a LJ fluid is plotted as a function of the reduced density for three isotherms. The relaxation times go through minima at $\rho^* \approx 0.7$ for all isotherms. The presence

Table I. Constants used in Eqs. (11) and (12) to Calculate the Shear Viscosity for LJ Fluids [25]

j	b_{j1}	b_{j2}	b_{j3}	b_{j4}	ω_j
1	−7.53814	36.0319	−47.0432	19.7791	2.8745
2	66.0342	−299.373	430.291	−191.670	−2.0265
3	−220.881	1067.97	−1575.25	725.006	0.1958
4	334.883	−1638.92	2445.08	−1140.09	−0.1960
5	−226.756	1112.30	−1669.43	783.084	0.0160
6	52.4394	−255.199	380.704	−176.589	–

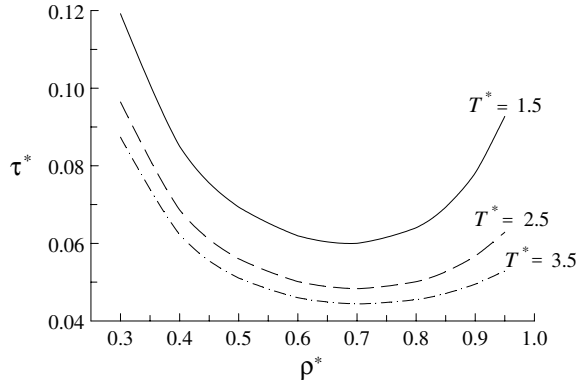

Fig. 5. Reduced shear relaxation time versus reduced density for three isotherms of LJ fluid.

of a common minimum is attributed to the unusual behavior of viscosity versus density isotherms in the supercritical region [25]. In the supercritical region, different viscosity isotherms intersect at a common density where the viscosity of the gas is independent of temperature. This behavior is shown in Fig. 6. The density of intersection point is about twice the critical density [26]. By comparing the density of the minima of Fig. 5 and the density of the common point in Fig. 6, it is observed that these two densities are very close to one another.

For practical applications, it is convenient to have an analytical expression for the density and temperature dependence of the shear relaxation time. Figure 5 shows that the general form of the τ^*–ρ^* isotherms are similar, and therefore the isotherms have a common functional dependence on temperature. Using a least-squares method, the reduced relaxation time

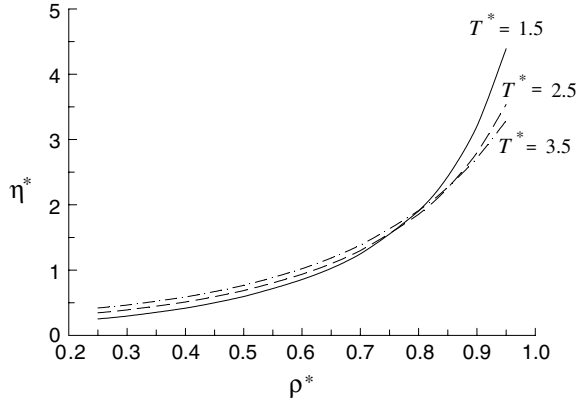

Fig. 6. Common point of the shear viscosity Lennard-Jones fluid for three isotherms, $T^* = 1.5$ (—), $T^* = 2.5$ (– –), and $T^* = 3.5$ (–·–).

of the LJ fluid can be fit to the following functional form:

$$\frac{\tau^*}{T^{*-0.3717}} = 0.859 - 5.5849\rho^* + 16.6395\rho^{*2} - 25.4717\rho^{*3} + 19.5756\rho^{*4} - 5.9341\rho^{*5}, \tag{14}$$

which is valid over the reduced density range of $0.25 < \rho^* < 0.90$ and the reduced temperature range of $1.5 < T^* < 4.0$. Equation (14) is plotted in Fig. 7 along with shear relaxation times calculated from viscosity points determined by MD simulations [25]. The MD points from different isotherms fall very close to the single curve. The discrepancies in the high-density range may be attributed to the inaccuracies of the MD viscosity results [25]. The maximum and average relative percent errors of Eq. (14) are 4.9 and 1.7%, respectively. This correlation provides an analytical expression in terms of ρ^* and T^* for the shear relaxation time.

Using molecular dynamics methods, Mountain and Zwanzig [9] reported that the order of the relaxation time for simple liquids is 10^{-13} s. This order of magnitude is consistent with our results. van der Gulik used thermal pressure to calculate the relaxation time for noble gases [10]. Although there is no strong indication that his methods will necessarily give the same relaxation time as obtained in this work, it is reassuring to see that the order of magnitude of the relaxation times are indeed identical for the case of argon and krypton given in Table II.

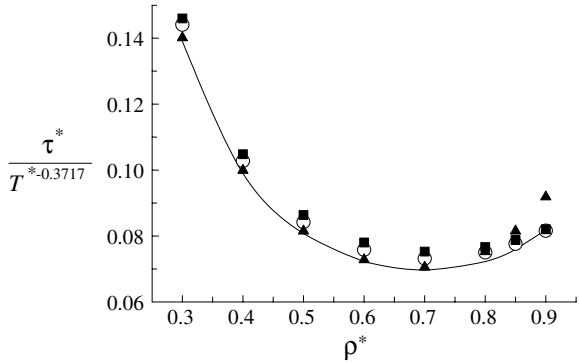

Fig. 7. Reduced relaxation time-temperature ratio as a function of reduced density for LJ fluids from Eq. (14) for $T^* = 2.5$ (—) and from MD simulations [25] for isotherms $T^* = 1.5$(▲), $T^* = 3.5$(○), and $T^* = 4$(■).

Table II. Comparisons of the Shear Relaxation Time using Eq. (14) for LJ Fluids and Eqs. (6) and (7) for SS Fluids with Experimental Values for Ar and Kr [10] where $\rho^* = \rho\sigma^3$ and $T^* = kT/\varepsilon$

	ρ^*	T^*	τ(ps)[a]	τ(ps)SS	τ(ps)LJ
Ar	0.511	2.493	0.47	0.27	0.11
	0.607	1.411	0.98	0.28	0.12
	0.623	1.131	2.2	0.29	0.13
	0.671	1.009	2.2	0.31	0.13
	0.767	0.863	2.1	0.38	0.14
Kr	0.652	1.697	0.79	0.37	0.14
	0.652	1.830	0.72	0.37	0.14
	0.683	1.565	0.89	0.39	0.15
Molecular Parameter	Ar	Kr	Molecular Parameter	Ar	Kr
σ	0.335 nm	0.3572 nm	ε/k	143.23	201.35

[a] From van der Gulik [10].

3.3. Relaxation Time for Argon as a Real Fluid

It is possible to consider argon as an example of a LJ fluid and to use Eq. (10) to predict its infinite shear modulus. Evaluation of relaxation time via Eq. (13) would then require an analytical expression for the viscosity of argon at different temperatures and densities. An analytical expression for the shear viscosity of supercritical fluids was presented in

our previous work [26,27],

$$\eta = \eta_0(1 + N_A\sigma^3 B_\eta^* \rho) + D\eta, \tag{15}$$

where η_0 is the Chapman–Enskog theory viscosity at zero density,

$$\eta_0 = \frac{5}{16}\left(\frac{mkT}{\pi}\right)\frac{f_\eta}{\sigma^2\Omega^{(2,2)*}(T^*)}, \tag{16}$$

m is the molecular mass, $\Omega^{(2,2)^*}(T^*)$ the reduced collisional integral, and f_η is the correlation factor [27]. B_η and D_η are the second viscosity virial coefficient and residual viscosity function, respectively, which are defined in Ref. 26. This analytical expression for the shear viscosity of real fluids is valid between $1.75 < T^* < 3.5$ and $0 < \rho^* < 0.991$. The reduced shear relaxation time for argon calculated using Eqs. (10) and (15) is shown in Fig. 8a. Figure 8a shows that for all isotherms, the relaxation time passes through a minimum at $\rho^* \approx 0.65$. It is remarkable that the minimum density is only weakly temperature dependent. The transition which gives rise to the minima will be further discussed in Section 4.

Finally, we have fitted the calculated values of the shear relaxation time of argon to the following correlation function:

$$\frac{\tau^*}{T^{*-0.2915}} = 0.7797 - 4.265\rho^* + 10.6098\rho^{*2} - 13.9324\rho^{*3} + 9.568\rho^{*4} - 2.5638\rho^{*5}. \tag{17}$$

The maximum and average relative percent error of this correlation function that were obtained from a least-squares method are 0.63 and 0.13%, respectively. The reduced density and temperature range of Eq. (17) is $0.25 < \rho^* < 0.95$ and $1.75 < T^* < 3.5$, respectively. Equation (17) has been used to plot the relaxation time for three isotherms in Fig. 9, which shows that the data points of the isotherms are superimposable on a single curve.

4. DISCUSSION

For soft spheres, the integral in the Mountain–Zwanzig expression for the infinite-frequency shear modulus G_∞^* in Eq. (2) has been solved numerically. For the soft-sphere potential, a corresponding states law for G_∞^* in terms of the variable $y \equiv (G_\infty^* - \rho^* T^*)/\rho^{*2}$ as a function of the variable $x = \rho\sigma^3(\varepsilon/kT)^{3/n}$ was written. Our comparison with the MD [19] results indicates the accuracy of this corresponding states behavior. Along with the Ashurst–Hoover expression for shear viscosity, this allows the derivation of an analytical expression for the shear relaxation time of SS fluids.

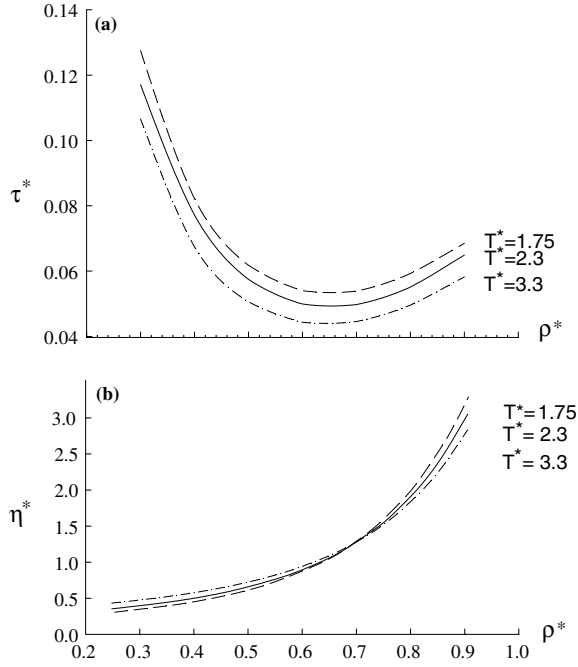

Fig. 8. (a) Reduced shear relaxation time versus reduced density for three isotherms of LJ fluid and (b) common point of the shear viscosity of argon for the same three isotherms shown in part (a) [26].

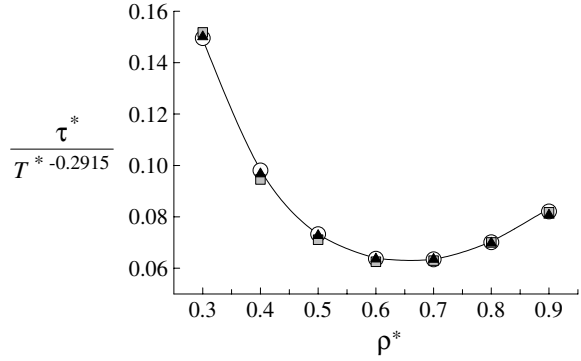

Fig. 9. Reduced relaxation time-temperature ratio versus reduced density for argon as a real fluid from Eq. (17) for the $T^* = 2.5$ (—) isotherm along with values from the viscosities at $T^* = 1.75$(▲), $T^* = 2.1$(○), and $T^* = 3.45$(□), Ref. 26.

The shear modulus G^*_∞ can also be determined numerically for the LJ potential by using the Matteoli–Mansoori RDF [24] and integration of Eq. (2). Our comparison with the MD results indicates the accuracy of this approach. Using Eq. (10) and an appropriate form for the shear viscosity over a wide temperature–density range, the shear relaxation time can be fit to an analytical function of temperature and density. It was shown in Fig. 7 that isotherms of the reduced relaxation time become superimposed on a single curve when plotted as a function of the reduced density in the form of Eq. (14).

In Figs. 3 and 7, the shear relaxation times for supercritical isotherms ($1.75 < T^* < 3.5$) of SS and LJ fluids pass through a minimum at $\rho^* \approx 0.70$. For the LJ fluid, a corresponding states law for the reduced relaxation time can be written (see Eq. (14)). This behavior of the relaxation time of LJ fluids can be attributed to the unusual "common density point" behavior of viscosity versus density seen in supercritical isotherms [27]. At high densities, the viscosity–density isotherms of gases generally intersect at a common point [27], (with density of ρ_{com}) at which the viscosity of the gas becomes independent of temperature (see Fig. 8b). This common point occurs at $\approx 2\rho_{\text{crit}}$, where ρ_{crit} is the critical density of the gas. The reduced critical density of Lennard–Jones fluids is 0.35 (for argon $\rho^*_{\text{crit}} = 0.32$) [28], therefore twice the reduced critical density is close to 0.70. At densities greater than ρ_{com}, the viscosity of gases decreases with increasing temperature, a behavior similar to that observed in liquids. Figures 8a,b show that the density of the minimum in the relaxation time and the common intersection point coincide closely.

In dilute gases, the most important mechanism for transporting momentum between layers of flowing fluid is the kinetic contribution. As the density of the fluid increases, the mean free path becomes shorter, and the total intermolecular potential on each particle becomes larger. At densities higher than the common point density, "collisional transfer" becomes the principle mechanism of viscosity [2,3,27] rather than the kinetic transfer, and therefore, the fluid behavior resembles that of liquids. The dominant mode of momentum transfer changes as the dense fluid passes through the common point density.

Both the viscosity and the shear modulus increase monotonically with temperature, but with different slopes; see, for example, Figs. 4 and 6. However, as seen from the result of Eq. (13) plotted in Fig. 8a, the relaxation time, which is the ratio of the viscosity and shear modulus, goes through a minimum. At densities lower than the common-point density, viscosity is dominated by the mean free path (dilute vapor behavior) mechanism, and kinetic transport and the rate of increase of the viscosity is not sufficient to overcome the rate of increase of the shear modulus.

Therefore, the relaxation time decreases with density. At densities larger than the common-point density ρ_{com}, the viscosity is dominated by collisional transfer (liquid-like behavior), which increases with density at a sharper rate than before, and as a result, the relaxation time begins to increase with density. The density of the minimum point is very close to the density of the common point which was reported in Ref. 27 to be about twice the critical density.

The minimum in the shear modulus can be interpreted from another point of view. We may describe the behavior of the relaxation time of a fluid in terms of the deformation of the fluid and its available translational states. At lower densities ($\rho^* < 0.70$), fluids show gas-like behavior, and even a very small force will be quickly transferred to the molecules and elastic deformation in the fluid is not observed. In this density region, the fluid is Newtonian and does not have memory of the deformation and cannot recall its previous shape. Hence, we conclude that translational states have a dominant role in the relaxation time in the gas-like region, so in this region energy and momentum of molecules easily distribute in translational states and this causes a decrease of the relaxation time.

In the dense region ($\rho^* > \rho^*_{\text{com}} \approx 0.70$), the fluid is viscoelastic and its behavior is influenced by finite memory effects which increase with density. The mechanism of the relaxation becomes similar to that in solids which have infinite memory on deformation and satisfy Hooke's law. An elastic solid will always recall its previous shape and relaxation is difficult to achieve. We may conclude that for densities greater than 0.70, the role of the memory effects are the dominant factor in comparison with accessible translational states and this causes an increase in the relaxation time. We are also able to predict the density where the momentum transfer mode goes from gas-like behavior to liquid-like behavior.

ACKNOWLEDGMENTS

The authors thank the referee of the earlier version of this manuscript for the comments. We wish to acknowledge the research council of Isfahan University of Technology for financial support (Grant No. 1CHA811).

REFERENCES

1. D. A. McQuarrie, in *Statistical Mechanics* (Harper and Row, New York, 1976).
2. S. Chapman and T. G. Cowling, in *The Mathematical Theory of Non-uniform Gases* (Cambridge University Press, 1939).
3. J. O. Hirschfelder, C. F. Curtiss, and R. B. Bird, in *Molecular Theory of Gases and Liquids* (Wiley, New York, 1954).

4. M. D. Magee, *J. Chem. Soc., Faraday Trans.2* **70**:929 (1974).
5. H. J. M. Hanley, J. C. Rainwater, and M. L. Huber, *Int. J. Thermophys*. **9**:1041 (1988).
6. S. Hess and H. J. M. Hanley, *Phys. Lett*. **98A**:35 (1983).
7. S. Hess, *Phys. Rev. A* **22**:2844 (1980).
8. H. J. M. Hanley, J. C. Rainwater, and S. Hess, *Phys. Rev. A* **36**:1795 (1987).
9. R. D. Mountain and R. Zwanzig, *J. Chem. Phys*. **44**:2777 (1966).
10. P. S. van der Gulik, *Physica A* **256**:39 (1998).
11. N. E. Hill, *Proc. Phys. Soc*. 13, **67**:149 (1954).
12. J. P. Rothstein and G. H. McKinley, *J. Non-Newtonian Fluid Mech*. **108**:275 (2002).
13. J. Cakl and I. Machac, *Collect. Czech. Chem. Commun*. **60**:1124 (1995).
14. R. Zwanzig and R. D. Mountain, *J. Chem. Phys*. **43**:4464 (1965).
15. D. M. Heyes and P. J. Aston, *J. Chem. Phys*. **100**:2149 (1994); D. M. Heyes, *ibid* **107**:1963 (1997).
16. J. P. Hansen and J. J. Weis, *Mol. Phys*. **23**:853 (1972).
17. J. N. Cape and L. V. Woodcock, *J. Chem. Phys*. **72**:976 (1980).
18. J. P. Hansen, *Phys. Rev. A* **2**:221 (1970).
19. D. M. Heyes. *J. Chem. Soc., Faraday Trans.2* **79**:1741 (1983); *ibid. Physica A* **146**:341 (1987).
20. W. T. Ashurst and W. G. Hoover. *Phys. Rev A*. **11**:658 (1975); *ibid*. *Phys. Rev. Lett*. **31**:206 (1979).
21. D. M. Heyes, *Phys. Rev. B* **37**:5677 (1988).
22. P. Borgelt and C. Hoheisel, *Phys. Rev. A* **42**:789 (1990).
23. D. Kivelson, M. G. Kivelson, and I. Openheim, *J. Chem. Phys*. **52**:1810 (1970).
24. E. Matteoli and G. A. Mansoori, *J. Chem. Phys*. **103**:4672 (1995).
25. R. L. Rowley and M. M. Painter, *Int. J. Thermophys*. **18**:1109 (1997).
26. B. Najafi, Y. Ghayeb, J. C. Rainwater, S. Alavi, and R. F. Snider, *Physica A* **260**:31 (1998).
27. B. Najafi, Y. Ghayeb, and G. A. Parsafar, *Int. J. Thermophys*. **21**:1011 (2000).
28. L. L. Lee, in *Molecular Thermodynamics of Nonideal Fluids* (Butterworths Pubs., Boston, 1988), p. 246.